JOURNAL OF MATERIALS SCIENCE 27 (1992) 2124–2130

Temperature dependence of microhardness and structure of ferroelectric copolymers of vinylidene fluoride

F. J. BALTÁ CALLEJA, C. SANTA CRUZ
Instituto de Estructura de la Materia, CSIC, Serrano 119, 28006 Madrid, Spain
A. GONZÁLEZ ARCHE, E. LÓPEZ CABARCOS
Departamento de Química-Física, Facultad de Farmacia, Universidad Complutense 28040 Madrid, Spain

Measurement of the microhardness (H) and X-ray investigation of melt-crystallized random copolymers of vinylidene fluoride with trifluorethylene containing 60 to 80 mol% VF_2 were carried out as a function of temperature. The results show that (i) at a given temperature H rapidly increases with VF_2 content; (ii) the Curie transition was found to involve an inflection point in the exponential temperature dependence of hardness; and (iii) at the Curie temperature (T_c) the ferroelectric crystals undergo reversibly a solid-state transformation, followed by the microhardness, to a non-polar (paraelectric) state showing a faster hardness decrease with increasing temperature above T_c. Changes in H with VF_2 content and temperature are discussed in the light of the lattice spacings of the ferro- and paraelectric phases and crystallinity values. The application of a relationship to account for correlations between mechanical properties and microstructure is considered.

1. Introduction

Evidence for ferroelectric to paraelectric phase transformations in random copolymers of vinylidene fluoride (VF_2) and trifluorethylene (F_3E) as revealed by wide-angle X-ray scattering (WAXS) and small-angle X-ray scattering (SAXS) has been reported in the last few years [1–13]. The conformation of these copolymers at low temperatures in their ferroelectric phase is the same as that in β-PVF_2 [14, 15] (Fig. 1), i.e. chains in a planar all-*trans* conformation packed in a pseudo-hexagonal lattice so that the dipoles are parallel to the *b*-axis. Above the Curie temperature this conformation changes into a disordered sequence of conformational isomers (tg, tḡ, tt) [6–8] as a result of the introduction of gauge bonds, which rotate around the chain axis so that the unit cell is no longer polar. On cooling down to room temperature the high-temperature phase does not fully go back to the original ferroelectric low-temperature phase but is partly transferred into a low-temperature non-polar phase [16]. Based on X-ray, i.r. and Raman results Tashiro and Kobayashi [17] have visualized this phase as a kind of superlattice structure consisting of an aggregation of polar microdomains, with all-*trans* zig-zag chains, which are in a considerably disordered state contributing to the observed broadening and diffuseness of the X-ray scattering patterns.

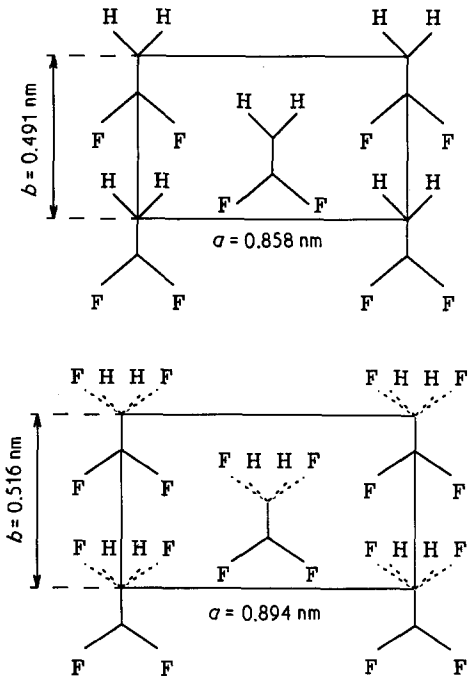

Figure 1 Unit cell projection along the molecular axis of β-PVF_2 (top) and of the ferroelectric phase of a 73–27 mol% VF_2–F_3E copolymer (bottom) [15].

The purpose of the present paper is to examine the behaviour of the mechanical properties of copolymers of VF_2 with F_3E through the Curie transition region as a function of temperature. The measurement of the microhardness (H) has proved to be a powerful method for the investigation of morphological and

0022–2461

microstructural changes in semicrystalline polymers [18, 19]. Furthermore, it is well known that the hardness of polymers can be directly correlated with many of their mechanical properties [18–22]. In particular, the use of H has also been proved to detect polymorphic changes in crystalline polymers [23] and phase transformations in amorphous solids including polymers [24, 25], in particular the glass transition behaviour. The specific aims of the present study are as follows:

1. To examine the influence of the concentration of VF_2 polar units along the chains for these copolymers on the mechanical property of microhardness.
2. To characterize the ferro- to paraelectric transition by measuring the microhardness as a function of temperature. Preliminary H–T data on the 70–30 copolymer have been reported previously [26].
3. To study whether the H variation is reversible with temperature or whether it presents a thermal hysteresis behaviour as occurs with other physical properties of these ferroelectric materials [27].
4. To explain the results in the light of structural considerations.

2. Experimental procedure

Commercial VF_2–F_3E copolymers from Atochem with compositions 60–40, 70–30 and 80–20 were pressure-moulded at temperatures between 160 and 180 °C to 100–200 μm thick films, and the films were subsequently quenched in ice water.

The microindentation hardness was measured using a square-based diamond and a loading cycle of 0.1 min. The microhardness value (in MPa) was derived from the residual projected impression using $H = kp/d^2$ where d is the mean diagonal length of the indentation in metres, p the applied force in Newtons and k a geometrical factor equal to 1.854. Loads of 0.15, 0.25, 0.5 and 1 N were used at room temperature. Elastic recovery of the samples after load removal was not detectable. The temperature dependence was determined in the 20–140 °C range using a hot stage with a heat controller designed by T. Yoshida, T. Asano and K. Mizuma at Shizuoka University. The surface temperature of the samples was calibrated with compounds of known melting point. During each measurement of H for each temperature, it was verified in a parallel measurement that the ferroelectric and paraelectric lattice spacings, as revealed by WAXS, remained constant. At high temperatures a load of 0.5 N was used. In order to obtain an adequate optical contrast of the impressions and to correct for possible elastic recovery a 10 nm thin layer of gold was evaporated on to the surface of the material. The hardness was measured during heating of the sample every 2–3 °C up to the neighbourhood of the melting point. It was found that H only depends on the temperature of measurement and is independent of the rate and time of heating up to times of 1 h. On cooling, the microhardness was measured every 5 °C down to room temperature.

3. Microhardness of semicrystalline polymers

3.1. Microhardness and its relation to structure parameters

To determine the plastic contribution to deformation, static indentation inducing the formation of a local surface impression (a few micrometres in size) is currently used [18]. The indentation stresses are highly concentrated in the plastic region immediately surrounding the contact area. Since the indentation process involves plastic yielding under the stress field of the indenter–once the stresses exceed the elastic limit–the microhardness is admittedly correlated with the specific modes of plastic deformation in the polymer. These involve at sufficiently large strains a cooperative destruction of crystalline lamellae [19, 20]. On the basis of a heterogeneous deformation model involving the generation of a number of shear planes within the plastically deformed crystals, we have developed a thermodynamic approach to account for the hardness dependence on the average thickness, l_c, of the crystalline lamellae [19]. In this concept the hardness of the crystals is described by

$$H_c = H_0/(1 + b/l_c) \quad (1)$$

where H_0 is the hardness value of an infinitely thick crystal and b is a parameter which is equal to twice the ratio of surface free energy to the enthalpy of crystal destruction. Experimental evidence for this model has been reported for different polymer systems (PE, PP, PET, PEO) (19, 20, 28–30). The range of b values obtained so far (b = 3–26 nm) is due to the different morphologies examined (chain-extended crystals, chain-folded lamellae, low-density PE, dry gel homopolymer and blended films, paraffins, etc). Since for flexible semicrystalline polymers above T_g

$$H \approx w_c H_c \quad (2)$$

where w_c is the crystallinity, the macroscopic hardness can be written as

$$H = \frac{w_c H_0}{1 + (b/l_c)} \quad (3)$$

If one further takes into account the exponential law-type decrease with temperature which has been found for the hardness of lamellar [31] and chain-extended morphologies [18] then

$$H = \frac{w_c H_0 e^{-\beta(T - T_a)}}{1 + (b/l_c)} \quad (4)$$

where β is the so-called coefficient of thermal softening of the material, and T_a is a reference temperature (usually room temperature). Equation 4 offers a general expression for the microhardness of a semicrystalline polymer at a given absolute temperature, T, having a mean crystal thickness l_c and a crystallinity w_c. Since yielding during indentation involves the plastic deformation of a large number of crystals, H, according to Equation 4, provides a good measure of the average crystal size. Let us discuss Equation 4 in

the following in the light of the structural parameters obtained for the VF_2 copolymers.

3.2. Temperature variation

In the temperature variation range between room temperature and the melting point of the polymer it is found that the crystallinity, w_c, for each copolymer remains nearly constant (Fig. 2). In addition, we also have found that the value of l_c remains constant in the low-temperature region, shows a stepwise increase at T_{Curie}, and remains constant again in the high-temperature region up to the neighbourhood of the melting point. Fig. 3 illustrates the X-ray long-period variations with temperature for the 6–40 copolymer. Since H_0 and b are constants one may assume that for these copolymers the quantity $w_c H_0/[1 + (b/l_c)]$ is a constant for each composition. Hence, according to Equation 4 for a given crystalline phase one can essentially expect an exponential variation of H as a function of T.

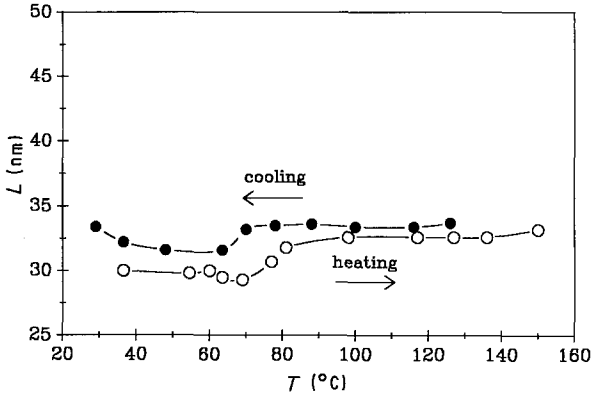

Figure 3 X-ray long period as a function of temperature during (○) heating up to the melt and (●) cooling down to room temperature for the 60–40 VF_2–F_3E copolymer.

In previous studies it was also shown that the decrease in H with temperature is a function of intermolecular distances within the crystals [31]. In other words, the decrease in H is directly related to the thermal expansion of the lattice. Fig. 4 illustrates as an example the variation of the lattice spacing for the 60–40 copolymer as a function of temperature. In the high-temperature region the spacing d_P of the paraelectric phase decreases linearly with temperature. At the Curie temperature ($T_c \sim 65\,°C$) a new spacing d_F corresponding to the ferroelectric phase appears and prevails in the low-temperature range. In addition, below T_{Curie} a small fraction (20%) of the initial paraelectric crystals is gradually transformed into a low-temperature non-ferroelectric phase having a spacing d_{NF}. The predominant ferroelectric spacing, d_F, follows a gradual final decrease with temperature. A similar behaviour of the lattice spacing with temperature has been observed for the other compositions [32]. In the discussion below an attempt will be made to describe the H results in the light of the main structural changes of these materials occurring as a function of temperature.

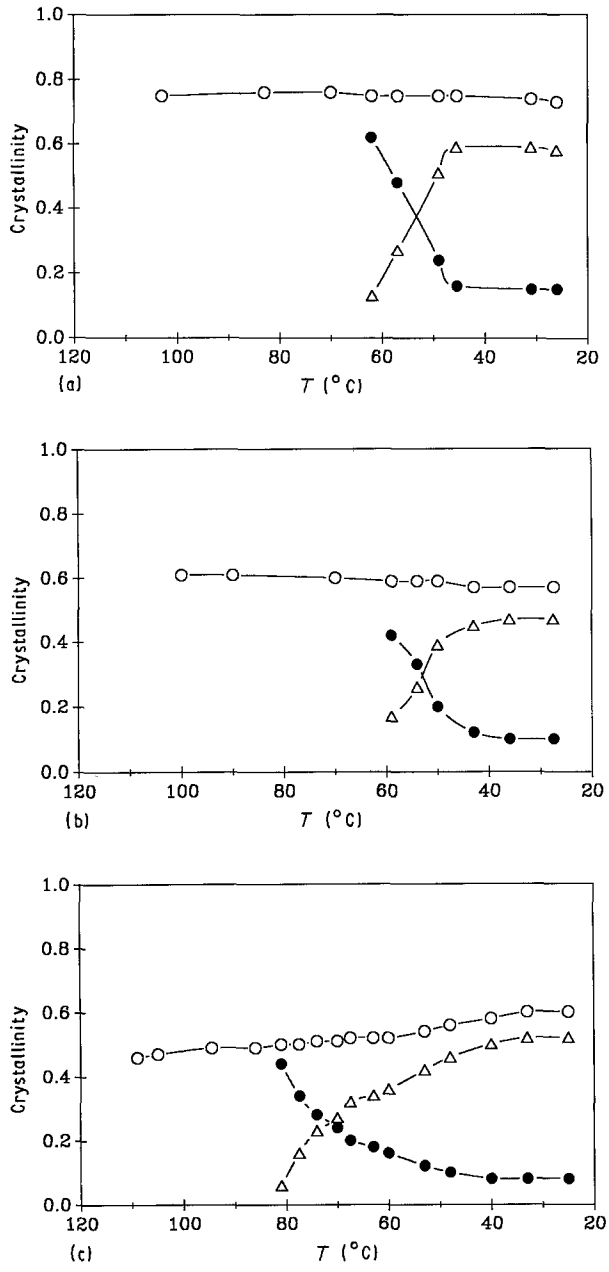

Figure 2 Variation of (○) total crystalline volume fraction x_c, and of crystalline fractions of (△) ferroelectric (x_c^F) and (●) non-ferroelectric (x_c^{NF}) crystals for (a) 60–40, (b) 70–30 and (c) 80–20 VF_2–F_3E copolymers as a function of decreasing temperature.

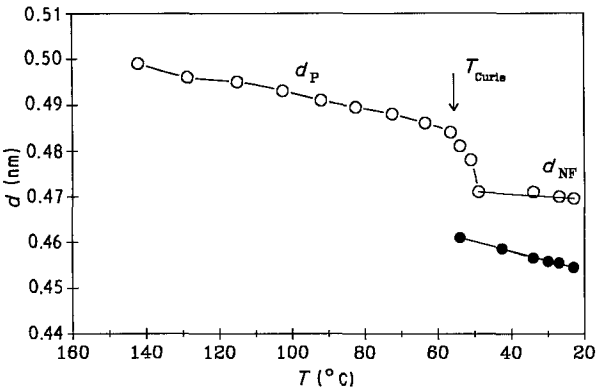

Figure 4 Variation of the lattice spacings of the 60–40 VF_2–F_3E copolymer as a function of decreasing temperature: (●) d_F, (○) d_{NF}, d_P.

3.3. Dependence of microhardness on VF_2 content

At a given temperature H_0 is related to the critical stress required for plastic deformation of a polymer crystal [18]. Thus, the applied compressive and shear stresses must overcome the cohesive forces between molecules to induce an irreversible deformation. One may roughly derive the ideal shear strength S_0 of the molecular crystal normal to the chain axis from the lateral surface free energy σ, if one assumes that a displacement between adjacent molecules by an amount of say $\delta l \sim 0.1$ nm is sufficient for lattice destruction [18]. This gives an estimate of the ultimate transverse shear stress per chain, $S_0 = \sigma/\delta l$, which is proportional to the hardness. Calculated values are not far off from experimental H data for various polymers [18]. Since

$$\sigma = A^{1/2}\Delta h_f \tau \qquad (5)$$

where A is the chain cross-section in the crystalline phase, Δh_f is the melting enthalpy and τ is a constant equal to 0.12 [33], H is consequently related to the unit cell dimension of the crystals. It is known that in VF_2–F_3E copolymers the intermolecular lattice spacing, d, in both the ferroelectric and paraelectric phases varies with the F_3E content [32]. One may hence expect a variation of H with the number of bulkier trifluorethylene groups.

4. Results and discussion

4.1. Low temperature range: influence of copolymer composition on microhardness

Fig. 5a shows the obtained H variation as a function of increasing temperature for the three investigated copolymers with 60–40, 70–30 and 80–20 VF_2–F_3E molar concentrations. Let us first restrict our discussion to the hardness behaviour in the low-temperature region; the higher-temperature range will be discussed further below. In all cases $\log H$ was observed to decrease linearly with increasing temperature. The onset of the Curie transition can be clearly identified with a bend in the $\log H$–T plot. On cooling (Fig. 5) H increases again with decreasing temperature, and the point at which the Curie transition is ended can again be identified with the change in slope of the plot. It is noteworthy that the onset of the Curie transition temperature, as determined from the measurement of hardness, is lower after cooling than during the heating process. This is due to the thermal hysteresis of the exothermic T_{Curie} peaks appearing after solidification at lower temperatures [27]. Fig. 6 illustrates the fit found between the Curie transition temperature as determined from microhardness and as measured by calorimetry. Only for the 80–20 composition is there a certain uncertainty in the correlation, due to the overlapping of the Curie temperature with the melting point.

Most interesting is the fact that H at room temperature (Fig. 5) appreciably increases with VF_2 content. Since the fraction of ferroelectric crystals is nearly constant ($w_c \simeq 0.5$–0.6) for the various compositions (see Fig. 2), the hardness increase at low temperature

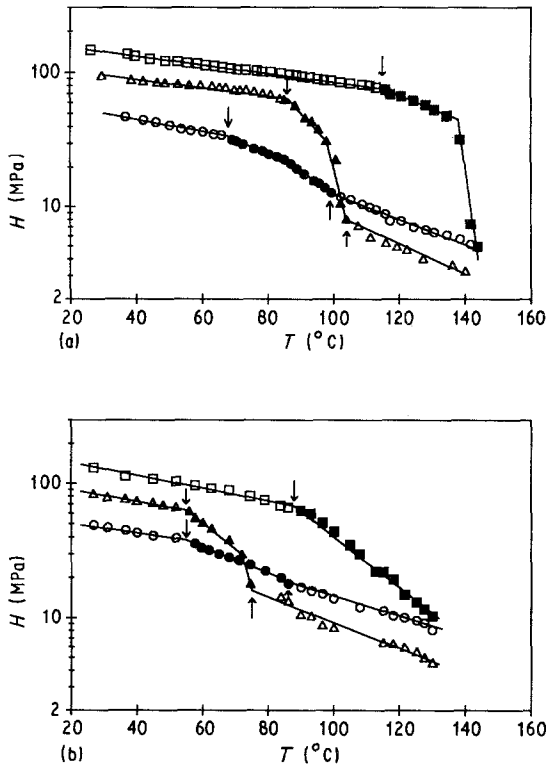

Figure 5 Temperature dependence of the microhardness during (a) heating and (b) cooling of the investigated copolymers: (○) 60–40, (△) 70–30, (□) 80–20 VF_2–F_3E.

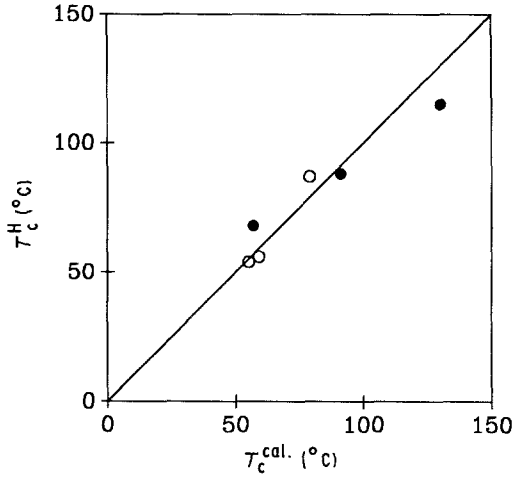

Figure 6 Correlation between the Curie temperatures (●) determined from microhardness and (○) measured by calorimetry.

can be explained on the basis of the structural characteristics of the ferroelectric phases of β-PVF_2 and its copolymers. In both cases the molecular conformation is the same. Intermolecular lattice structure, chain packing and dipolar alignment are also the same. The major difference between PVF_2 and its copolymers involves the spacing of their intermolecular lattice. In addition, in β-PVF_2 the dipole moments of the individual segments with a *trans* conformation reinforce each other, while in the case of its copolymers the dipole moments from the $-CF_2$ groups are partially compensated with the moments of the –CFH groups which are randomly distributed along the opposite side of the chain.

As is seen in Fig. 1, the a and b axes of the unit cell are significantly expanded in the copolymers because of the presence of additional fluorine atoms in trifluoroethylene. As a result of this lattice expansion the VF_2 units in the copolymers will not be in close contact, contrary to the situation in the β-PVF_2 homopolymer. In β-PVF_2 the 0.491 nm spacing is determined by the closest possible chain packing in the b direction. Since this is also the dipolar direction, the chains are held together by strong attractive forces so that any intramolecular rotation will be sterically hindered. In the copolymers, on the other hand, the separation between chains along the b direction increases with increasing CFH units randomly located along the chain axis. In addition, with increasing F_3E sequences the overall dipole moment within the ferroelectric crystal will diminish. As a result, the crystal hardness (the critical stress to irreversibly deform the crystals) decreases with increasing CFH units and shows a maximum value for the homopolymer, which presents the smallest unit cell and closest chain packing. Fig. 7 illustrates the linear increase of the crystal hardness with increasing unit cell density of the copolymers in the ferroelectric phase, including the highest H_c value found for the PVF_2 homopolymer.

4.2. High temperature range: Curie transition and microhardness of paraelectric crystals

To characterize fully the H behaviour of the paraelectric phase it is necessary to discuss the temperature range investigated up to higher temperatures. Fig. 5 also illustrates the H variation observed up to the vicinity of the melting temperature. For simplicity it is convenient to describe the changes in $\log H$ in the light of the results obtained with the 60–40 and 70–30 copolymers during heating. In both cases one may distinguish three to four different regions in the $\log H$–T plot, suggesting the presence of different structural mechanisms. The lowest and highest temperature regions correspond to the thermal expansion of the ferroelectric and paraelectric crystalline phases, respectively (open symbols) and are characterized by

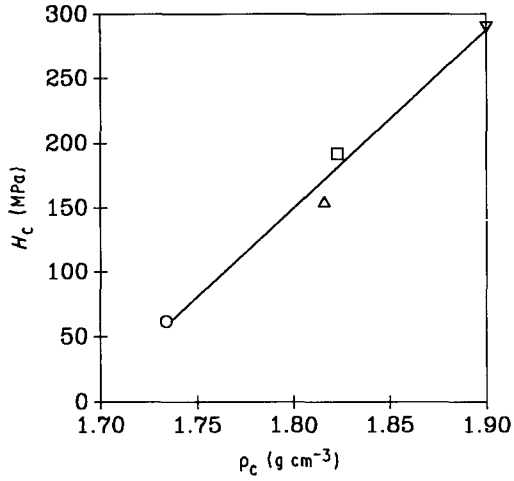

Figure 7 Variation of crystal hardness as a function of unit cell density for the various VF_2–F_3E compositions: (○) 60–40, (△) 70–30, (□) 80–20, (▽) PVF_2.

two thermal softening coefficients β_F and β_P. Within the Curie transition region (solid symbols) the presence of two further slopes in the $\log H$–T plot could be inferred. These two regions might be associated with the doublets appearing in the calorimetric scans observed in the Curie transition region [12]. The faster decreases in H beginning at ~ 90 °C for the 70–30 copolymer and at 70 °C for the 60–40 copolymer suggests the presence of drastic changes in structure. To explain the first slope (90–100 °C interval for the 70% VF_2 copolymer) one might suggest a transition mechanism from the ferroelectric to the non-polar phase. For the second slope (100–105 °C region for the 70% VF_2 copolymer) one might think of a transition from the non-polar phase to the final high-temperature paraelectric phase. In the case of the 80–20 copolymer, in addition to the initial H decrease corresponding to the thermal expansion of the ferroelectric phase, one observes the onset of the Curie transition at about 115 °C which is then masked by the melting of the first crystals.

On cooling, the opposite behaviour of the microhardness, an increase with decreasing temperature, is observed (Fig. 5b). However, the Curie transition temperatures, as pointed out above, are shifted towards lower temperatures. Table I collects the coefficients of thermal softening for the different copolymers in the ferroelectric low-temperature phase and in the paraelectric high-temperature phase. For $T < T_{Curie}$ it is found that $\beta_F \sim 10^{-2}\ K^{-1}$, which is of the same order of magnitude as that obtained for the crystalline phase in other polymers [18, 31, 34]. On the other hand, for $T > T_{Curie}$, H decreases at a larger rate ($\beta_P \sim 2 \times 10^{-2}\ K^{-1}$). This is most probably due to both a lack of the dipole alignment in the chains containing a disordered arrangement of tg ± sequences, and to the existence of a larger intermolecular separation within the paraelectric crystals than in the ferroelectric phase. This is in accordance with the fact that the lattice expansion coefficient is larger in the former (paraelectric) than in the latter phase.

From the foregoing one may suggest the occurrence of a "liquid crystalline"-like state for the paraelectric material which, in fact, yields β_P values which are similar to those reported for amorphous polymers above T_g [25] and H values which are as low as those found for short-chain n-paraffins (n = 20–32) [34]. Furthermore, for $T > T_{Curie}$ in Fig. 5, it is found that, contrary to the room-temperature behaviour, H for the 70–30 paraelectric copolymer presents lower values than H for the 60–40 material. This finding may be connected with the fact that the volume fraction of the

TABLE I Coefficient of thermal softening, β, for VF_2–F_3E copolymers

Composition	β (× $10^3\ K^{-1}$)	
	$T < T_{Curie}$	$T > T_{Curie}$
60–40	9	17
70–30	9.5	22
80–20	11	45

paraelectric "crystals" is larger for the 60–40 copolymer ($w_c \sim 0.8$) than for the 70–30 composition ($w_c \sim 0.6$) (see Fig. 2).

4.3. Crystal density dependence

Fig. 8 illustrates the dependence of the crystal hardness on the crystal density for the samples investigated. This plot allows us to separate the two distinct contributions to H_c: (i) a gradual lattice contraction and (ii) a drastic change from the para- to the ferroelectric phases during cooling. At high temperature the paraelectric crystals show very low H_c values ($H_c \sim 10$ MPa). During cooling, lattice contraction takes place (ρ_c increases continuously) and H_c for each copolymer gradually increases. At the Curie transition the crystal density, ρ_c, for the 70–30 and 80–20 compositions suffers a discontinuous increase contributing to a slight H_c increase. For the 60–40 composition one observes at the Curie transition only an inflection point in the H_c–ρ_c plot. In the ferroelectric phase the lattice contracts further on cooling for the three copolymers, giving rise to a very steep crystal hardness increase with increasing crystal density.

4.4. Hysteresis behaviour

We wish to discuss the H behaviour of each copolymer, concerning the question of whether H varies reversibly with temperature. Fig. 9 illustrates the evolution of a H–T cycle during heating and cooling for the 70–30 copolymer. The fact that on cooling the Curie temperature range is shifted towards lower temperatures leads to a corresponding shift of the paraelectric phase lower boundary from 105 °C down to 75 °C. Within the Curie region H increases further up to the inflection point near $T = 55$ °C where the ferroelectric phase is restored. However, the slightly lower H values found after solidification could suggest the persistence of certain conformational tg, tḡ sequences anchored within the ferroelectric crystals which reduce dipole alignment within the chains and which are finally removed at room temperature. A similar hysteresis behaviour is hinted at for the 60–40

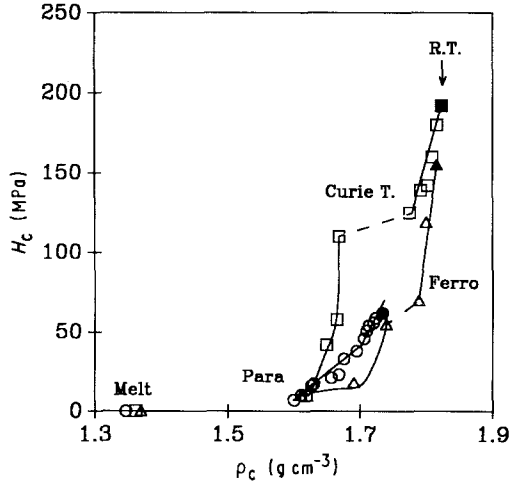

Figure 8 Dependence of crystal hardness upon unit cell density through the Curie transition.

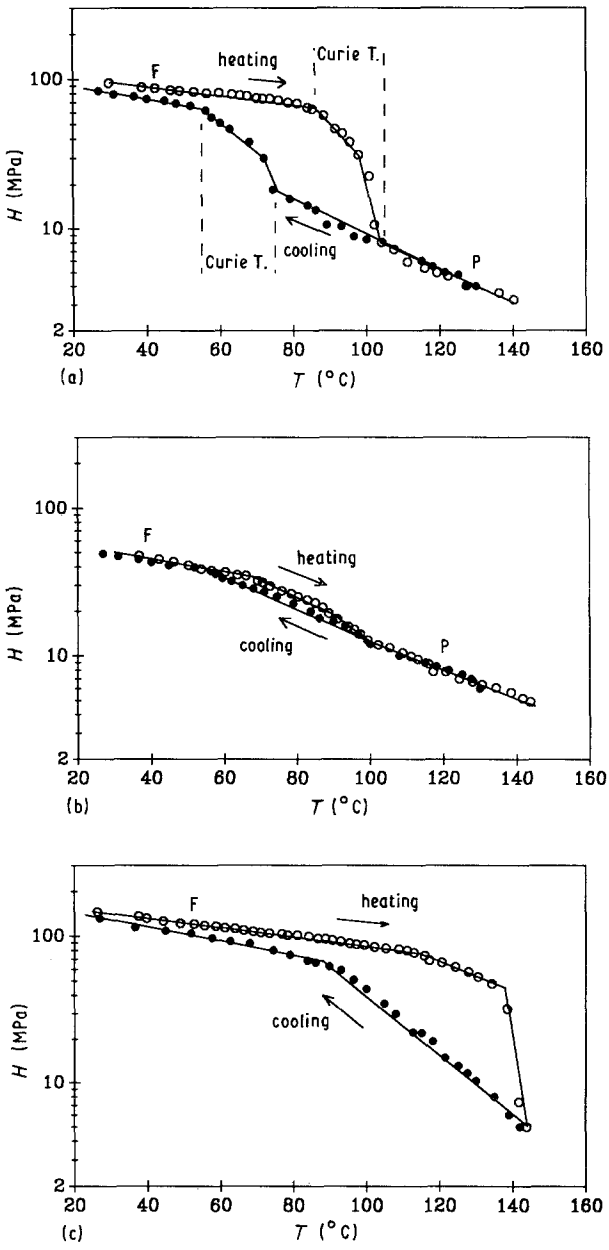

Figure 9 Thermal hysteresis behaviour of log H versus T for (a) 70–30, (b) 60–40, (c) 80–20 VF_2–F_3E compositions.

copolymer, though the H changes are very small in this case. In case of the 80–20 copolymer the hysteresis H curve cannot be fully obtained due to the superposition of the Curie transition and the melting of crystals beyond $T = 140$ °C. Here, during solidification the H increase from 140 °C down to about 100 °C is the result of a double contribution of (a) crystallization of the fraction of molten crystals and (b) thermal contraction of the non-polar phase crystals. Here, again, due to the shift in the Curie temperature, the ferroelectric phase is restored at 90 °C (instead of 115 °C). The lower H values found for the ferroelectric crystals on cooling below 90 °C suggest again the presence of conformational lattice defects which are eventually removed at room temperature.

5. Conclusions

Microhardness has been shown to be an appropriate technique to accurately detect ferroelectric to paraelectric phase changes in VF_2–F_3E copolymers. At

room temperature the increase in microhardness as a function of increasing VF_2 polar sequences has been correlated with the contraction of the unit cell and the parallel reduction in the number of dipoles, due to a decrease of bulky trifluorethylene units within the ferroelectric crystals. The microhardness of these materials when measured over a temperature range shows the following behaviour. At low temperatures (below T_c) the ferroelectric crystals follow an exponential decrease as a function of temperature, characterized by a thermal softening coefficient $\beta_F \approx 0.01\ K^{-1}$ similar to that found in other crystalline polymers in the same temperature range. At the Curie temperature the microhardness shows a sharp decrease on a plot of log H versus T, which characterizes a transition from the ferroelectric to the paraelectric phase involving a complex molecular reorganization within the crystals. At higher temperatures (above T_c) the paraelectric crystals present a much faster exponential H decrease with T which is characterized by a coefficient $\beta_P \approx 0.2$–$0.45\ K^{-1}$ similar to that of amorphous polymers above T_g, suggesting the existence of a "liquid crystalline" state. Finally, the study of the hardness of these materials during heating and cooling cycles reveals the existence of a hysteresis behaviour of the hardness with temperature which is caused by a shift in T_{Curie} towards lower temperatures during the cooling process.

Acknowledgements

The authors wish to express their thanks to T. Asano and T. Yoshida, Shizuoka University, for making available the hot stage for the microhardness measurements as mentioned in the text. Grateful acknowledgement is also due to CICYT, Spain (grant MAT88-0159), to the Internationales Büro, Kernforschunganlage, Karlsruhe, and to CSIC, Madrid for generous support of this investigation.

References

1. K. TASHIRO, K. TAKANO, M. KOBAYASHI, Y. CHATANI and H. TADOKORO, *Polymer* **22** (1981) 1312.
2. T. FURUKAWA, G. E. JOHNSON, H. E. BAIR, Y. TAJITSU, A. CHIBA and E. FUKADA, *Ferroelectrics* **32** (1981) 61.
3. Y. HIGASHIHATA, J. SAKO and T. YAGI, *ibid.* **32** (1981) 85.
4. A. J. LOVINGER, G. T. DAVIES, T. FURUKAWA and M. G. BROADHURST, *Macromolecules* **15** (1982) 323.
5. G. T. DAVIES, T. FURUKAWA, A. J. LOVINGER and M. G. BROADHURST, *ibid.* **15** (1982) 329.
6. A. LOVINGER, T. FURUKAWA, G. T. DAVIS and M. G. BROADHURST, *Polymer* **24** (1983) 1225.
7. *Idem., ibid.* **24** (1983) 1233.
8. K. TASHIRO, M. NAKAMURA, M. KOBAYASHI, M. CHATANI and H. TADOKORO, *Macromolecules* **17** (1984) 1452.
9. M. V. FERNÁNDEZ, A. SUZUKI and A. CHIVA, *ibid.* **20** (1987) 1806.
10. E. LOPEZ CABARCOS, A. GONZALEZ ARCHE, J. MARTÍNEZ SALAZAR and F. J. BALTÁ CALLEJA, in "Integration of fundamental science and technology", edited by P. J. Lemstra and A. K. Kleintjens (Elsevier, 1988) p. 415.
11. E. LÓPEZ CABARCOS, A. GONZÁLEZ ARCHE, F. J. BALTÁ CALLEJA and H. G. ZACHMANN, *Makromol. Chem. Makromol. Symp.* **20/21** (1988) 193.
12. H. MARAND and R. S. STEIN, *Macromolecules* **22** (1989) 444.
13. J. F. LEGRAND, *Ferroelectrics* **91** (1989) 303.
14. R. HASEGAWA, Y. TAKAHASHI, Y. CHATANI and H. TADOKORO, *Polym. J.* **3** (1972) 600.
15. A. LOVINGER, *Macromolecules* **18** (1985) 910.
16. K. TASHIRO, K. TAKANO, M. KOBAYASHI, Y. CHATANI and H. TADOKORO, *Polymer* **25** (1984) 195.
17. K. TASHIRO and M. KOBAYASHI, *ibid.* **27** (1985) 67.
18. F. J. BALTÁ CALLEJA, *Adv. Polym. Sci.* **66** (1985) 117.
19. F. J. BALTÁ CALLEJA and H. G. KILIAN, *Colloid Polym. Sci.* **263** (1985) 697.
20. *Idem., ibid.* **266** (1988) 29.
21. B. DARLIX, B. MONAISE and P. MONTMITONETT, *Polym. Testing* **6** (1986) 107.
22. B. MARTIN, J. M. PEREÑA, J. M. PASTOR and J. A. SAJA, *J. Mater. Sci. Lett.* **5** (1986) 1027.
23. F. J. BALTÁ CALLEJA, J. MARTÍNEZ SALAZAR and T. ASANO, *ibid.* **7** (1988) 165.
24. S. O. KASAP, S. YANNACOPOULOS and P. GUNDAPPA, *J. Non-Cryst. Solids* **111** (1989) 82.
25. F. ANIA, J. MARTÍNEZ SALAZAR and F. J. BALTÁ CALLEJA, *J. Mater. Sci.* **24** (1989) 2934.
26. J. MARTÍNEZ SALAZAR, J. C. CANALDA, E. LÓPEZ CABARCOS and F. J. BALTÁ CALLEJA, *Colloid Polym. Sci.* **266** (1988) 41.
27. K. KOGA and H. OHIGASHI, *J. Appl. Phys.* **59** (1986) 2142.
28. F. J. BALTÁ CALLEJA, C. SANTA CRUZ, R. K. BAYER and H. G. KILIAN, *Colloid Polym. Sci.* **268** (1990) 440.
29. F. J. BALTÁ CALLEJA, C. SANTA CRUZ, C. SAWATARI and T. ASANO, *Macromolecules* **23** (1990) 819.
30. C. SANTA CRUZ, F. J. BALTÁ CALLEJA, H. G. ZACHMANN, N. STRIBECK and T. ASANO, *J. Polym. Sci. Phys. Polym.* **29** (1991) 819.
31. J. MARTINEZ-SALAZAR, J. GARCIA PEÑA and F. J. BALTA CALLEJA, *Polym. Commun.* **26** (1985) 57.
32. A. GONZÁLEZ ARCHE, PhD thesis, Universidad Complutense, Madrid (1990).
33. D. G. THOMAS and L. A. K. STAVELY, *J. Chem. Soc.* (1952) 4569.
34. F. ANIA, H. G. KILIAN and F. J. BALTÁ CALLEJA, *J. Mater. Sci. Lett.* **5** (1986) 1183.

Received 20 December 1990
and accepted 13 May 1991